

1 **Characterization and diversification of AraC/XylS family regulators guided by transposon**  
 2 **sequencing**

3  
 4 Allison N. Pearson<sup>1,2,3,\*</sup>, Matthew R. Incha<sup>1,2,3,\*</sup>, Cindy Ho<sup>1,2</sup>, Matthias Schmidt<sup>1,2,4</sup>, Jacob B.  
 5 Roberts<sup>1,2,5</sup>, Alberto A. Nava<sup>1,2,6</sup>, Jay D. Keasling<sup>1,2,5,6,7,8,9,#</sup>

6  
 7 <sup>1</sup>Joint BioEnergy Institute, 5885 Hollis Street, Emeryville, CA 94608, USA.

8 <sup>2</sup>Biological Systems & Engineering Division, Lawrence Berkeley National Laboratory, Berkeley,  
 9 CA 94720, USA.

10 <sup>3</sup>Department of Plant and Microbial Biology, University of California, Berkeley, CA 94720, USA

11 <sup>4</sup>Institute of Applied Microbiology-iAMB, Aachen Biology and Biotechnology-ABBt, RWTH  
 12 Aachen University, Aachen, Germany

13 <sup>5</sup>Joint Program in Bioengineering, University of California, Berkeley/San Francisco, CA 94720,  
 14 USA

15 <sup>6</sup>Department of Chemical and Biomolecular Engineering, University of California, Berkeley, CA  
 16 94720, USA

17 <sup>7</sup>Institute for Quantitative Biosciences, University of California, Berkeley, CA 94720, USA

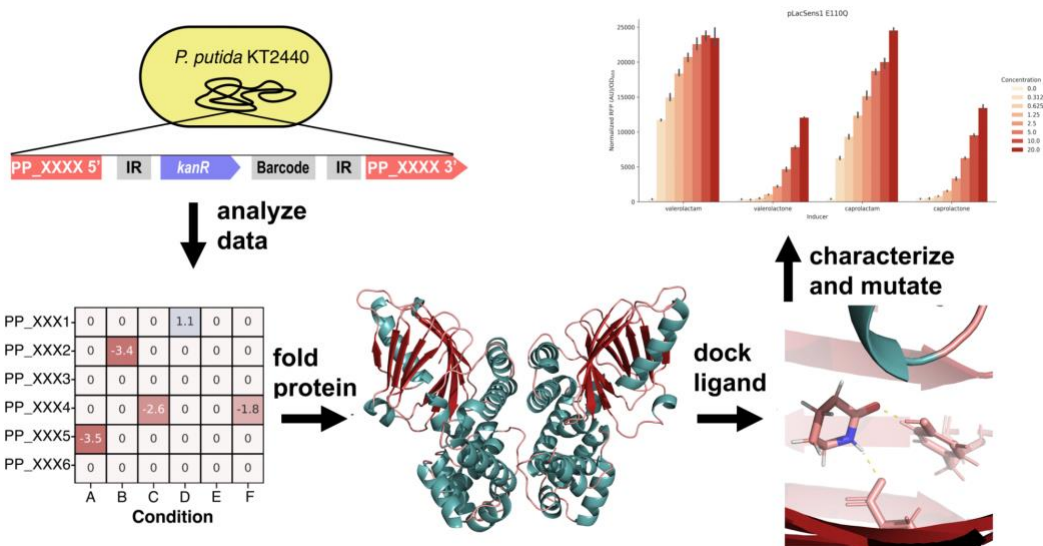
18 <sup>8</sup>The Novo Nordisk Foundation Center for Biosustainability, Technical University of Denmark,  
 19 Denmark

20 <sup>9</sup>Center for Synthetic Biochemistry, Institute for Synthetic Biology, Shenzhen Institutes for  
 21 Advanced Technologies, Shenzhen, China

22  
 23 \*Authors contributed equally. Author order was determined by a D20 dice roll. ANP rolled a  
 24 natural 20 and MRI rolled a 7.

25  
 26 #Corresponding author  
 27 Jay D. Keasling, [jdkeasling@lbl.gov](mailto:jdkeasling@lbl.gov)  
 28

29 **Graphical Abstract:**



1 **Abstract:**

2 In this study, we explored the development of engineered inducible systems. Publicly available  
3 data from previous transposon sequencing assays were used to identify regulators of  
4 metabolism in *Pseudomonas putida* KT2440. For the AraC-family regulators (AFRs)  
5 represented in this data, we posited AFR/promoter/inducer groupings. Eleven promoters were  
6 characterized for a response to their proposed inducers in *P. putida*, and the resultant data were  
7 used to create and test nine two-plasmid sensor systems in *E. coli*. Several of these were  
8 further developed into a palette of single-plasmid inducible systems. From these experiments,  
9 we observed an unreported inducer response from a previously characterized AFR,  
10 demonstrated that the addition of a *P. putida* transporter improved the sensor dynamics of an  
11 AFR in *E. coli*, and identified an uncharacterized AFR with a novel potential inducer specificity.  
12 Finally, targeted mutations in an AFR, informed by structural predictions, enabled further  
13 diversification of these inducible plasmids.

14

15 **Introduction:**

16 Rapid screening to optimize biosynthetic performance requires a method that can keep  
17 pace with process development. An allosteric transcription factor (aTF)-based biosensor can fill  
18 this need by using a fluorescent or selectable marker to quickly screen or select high-performing  
19 variants. The success of this method depends on using known aTFs with established ligands or  
20 engineering an aTF to respond to a new ligand <sup>1-3</sup>. To increase probability of success,  
21 researchers should start the aTF engineering process with a well-characterized protein that has  
22 a similar ligand to the desired biochemical <sup>4</sup>.

23 AraC/XylS-family regulators (AFRs) have shown potential as biosensors and inducible  
24 systems, due to their ability to be engineered for specific ligand recognition and previous  
25 successful applications in synthetic biology and metabolic engineering <sup>5-7</sup>. AFRs are commonly  
26 found in bacteria; the most well-known and characterized are the canonical arabinose (AraC-

1 P<sub>BAD</sub>) and xylose (XylS-P<sub>xyIM</sub>) inducible systems of *Escherichia coli* and *Pseudomonas putida*,  
2 respectively, which lend the family its name<sup>8–10</sup>. A repertoire of inducible AFRs would benefit  
3 bioengineering and molecular biology, each potentially offering unique benefits in terms of  
4 ligand cost or induction dynamics. Additionally, a high-throughput method for identifying these  
5 regulators would advance the development of customized inducible systems and biosensors.

6 Randomly barcoded transposon-site sequencing (RB-TnSeq) has proven effective in  
7 identifying key genes associated with metabolic pathways and stress responses. In our previous  
8 studies, we performed 206 RB-TnSeq assays on a mutant library of *Pseudomonas putida*  
9 KT2440, revealing significant phenotypes in over 1000 genes. By analyzing these data and  
10 drawing from database annotations, we have discovered specific functions such as substrate  
11 preferences for genes with multiple paralogs<sup>11–14</sup>. In these datasets we have also identified  
12 numerous transcription factors with significant fitness phenotypes that may provide evidence for  
13 their ligand specificities and target regulons<sup>14</sup>.

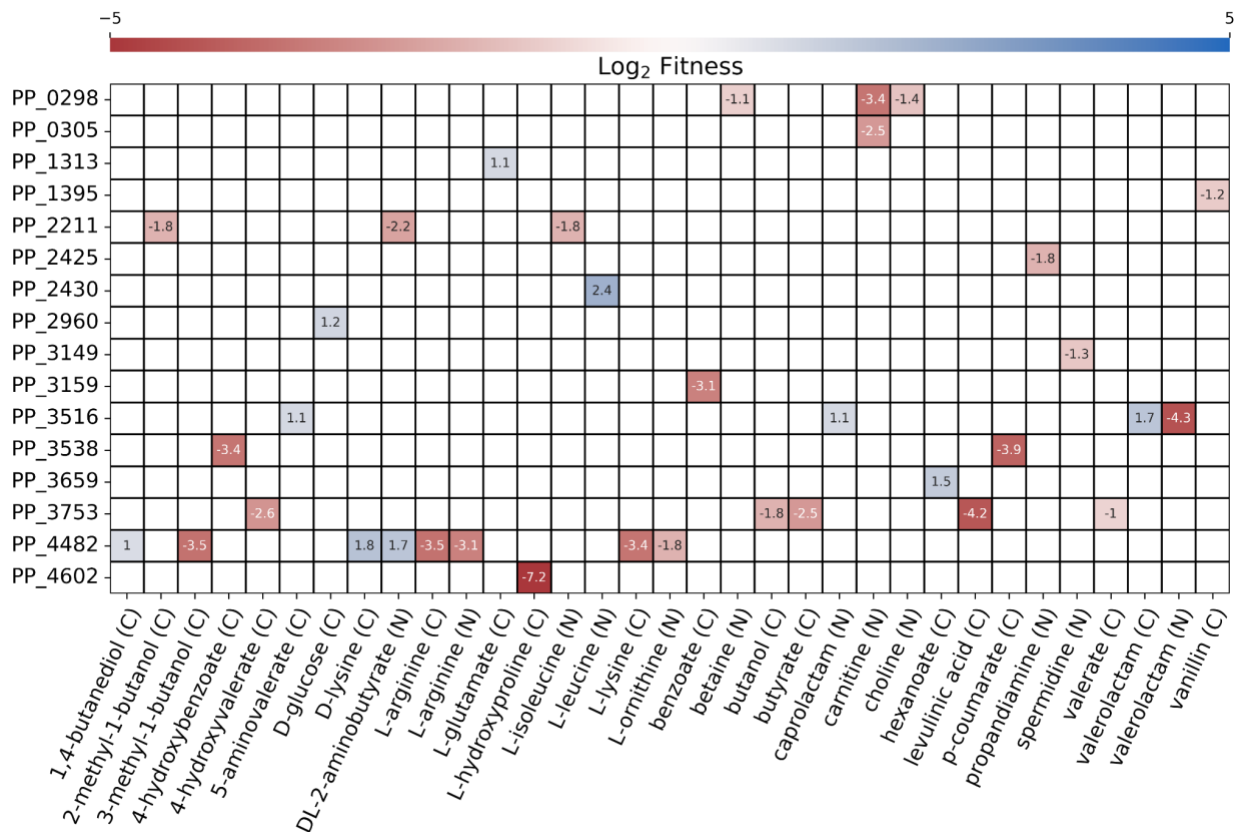
14 The advancement of new protein structure prediction tools could further accelerate  
15 development of inducible systems with more diverse ligand responses through rational  
16 mutagenesis. Previous studies have relied on known protein structures or homology models of  
17 transcription factors for rational engineering<sup>2</sup>. However, AlphaFold2 and RosettaFold present a  
18 new method of protein structure prediction that can elucidate structures with high fidelity<sup>15,16</sup>.  
19 Coupling AlphaFold2 structural predictions and rational mutagenesis with RB-TnSeq methods of  
20 gene identification has yet to be described, but we believe this presents a powerful new  
21 approach for the creation of novel inducible systems.

22 In this study, we investigated nine AFRs represented in public RB-TnSeq data. These  
23 regulators and their promoters were characterized, and single- and two- plasmid inducible  
24 systems were created and tested in *Escherichia coli*. Through these assays, we constructed  
25 functional inducible promoters from a new uncharacterized AFR with novel ligand specificity, as  
26 well as 2 other AFRs represented in the datasets. We made targeted mutations in the binding

1 pockets of three AFRs guided by AlphaFold structure predictions and modified their activities.  
2 This demonstrates the usefulness of functional genomics and *in silico* approaches in developing  
3 new inducible systems for controlling cell function. Many additional regulators from different  
4 families, including the LysR, GntR, GerE/LuxR, and IclR families, also have significant fitness  
5 changes in publicly available RB-TnSeq datasets<sup>17–20</sup>. We believe future work could employ  
6 these other transcription factors represented in RB-TnSeq datasets to generate more diverse  
7 inducible systems.

8

## 9 Results:



10

11 Figure 1. Fitness data for AraC family transcription regulators with significant fitness changes ( $|t$ -  
12 score  $> 4$ ,  $|\text{fitness}| > 1$ ). Fitness changes that did not meet the cutoff are not shown.

13

14

15

## 1 **Phenotypic identification of AraC family regulators**

2 *Pseudomonas putida* KT2440 carries 40 distinct AraC/XylS family regulators (AFRs) in  
 3 its genome, based on a search of the genome for proteins containing the conserved AFR helix-  
 4 turn-helix domain, Pfam HTH\_18 (PF12833)<sup>21</sup>. Some have known or predicted functions;  
 5 however, others lack a specific annotation. Through analyzing barcode transposon abundance  
 6 sequencing (RB-TnSeq) data, we found 16 AFRs with significant ( $|t\text{-score}| > 4$ ,  $|fitness| > 1$ )  
 7 phenotypes (Figure 1)<sup>14,22,23</sup>. The regulator OplR (PP\_3516) was previously identified via  
 8 proteomics and later was shown to have a significant phenotype in a nitrogen-source RB-TnSeq  
 9 dataset<sup>11-14</sup>. Other AFRs present in the data, such as gbdR (PP\_0298), cdhR (PP\_0305), benR  
 10 (PP\_3159), pobR (PP\_3538), and argR (PP\_4482), either have predicted functions based on  
 11 homology or have been previously characterized and align with our fitness data<sup>24-28</sup>. Based on  
 12 prior literature, co-fitness, and/or proximity to other metabolic genes, we assigned regulon  
 13 predictions for 9 of the 16 AFRs in the data (Table 1).

14

15 Table 1. Promoters, predicted transcriptional regulators, and predicted in-vivo ligands for each  
 16 system tested in this study, along with the fold induction between the maximum measured  
 17 normalized RFP values and the uninduced controls. n=3, error = standard deviation.

Predicted AFR	Predicted target promoter	Predicted <i>in vivo</i> ligands	Tested ligands	Fold induction of promoters in <i>P. putida</i>
PP_0298 (gbdR)	P <sub>PP_0296</sub>	betaine	betaine	2.2 ± 0.26
PP_0305 (cdhR)	P <sub>PP_0304</sub>	carnitine	carnitine	270 ± 13
PP_3149	P <sub>PP_3148</sub>	spermidine	spermidine	67 ± 8.5
PP_3538 (pobR)	P <sub>PP_3537</sub>	4-hydroxybenzoate	4-hydroxybenzoate	160 ± 31
PP_3753	P <sub>PP_3754</sub>	3-hydroxybutyrate, or 3-hydroxyvalerate	3-hydroxybutyrate levulinic acid	1.3 ± 0.32 6.9 ± 0.65
PP_4602	P <sub>PP_1259</sub>	L-hydroxyproline	L-hydroxyproline	310 ± 41
PP_3159 (benR)	P <sub>PP_3161</sub>	benzoate	benzoate	38 ± 5.2
PP_3159 (benR)	P <sub>PP_3160</sub>	benzoate	benzoate	1.7 ± 0.20
PP_4482	P <sub>PP_4486</sub>	L-arginine	L-arginine	6.5 ± 0.24

PP_4482	P <sub>PP_4481</sub>	L-arginine	L-arginine	11 ± 2.1
PP_2211	P <sub>PP_2213</sub>	2-methylbutyrate, or 2-methylbutyryl-CoA	2-methylbutyrate 2-methylbutanol	52 ± 4.7 19 ± 0.62

1

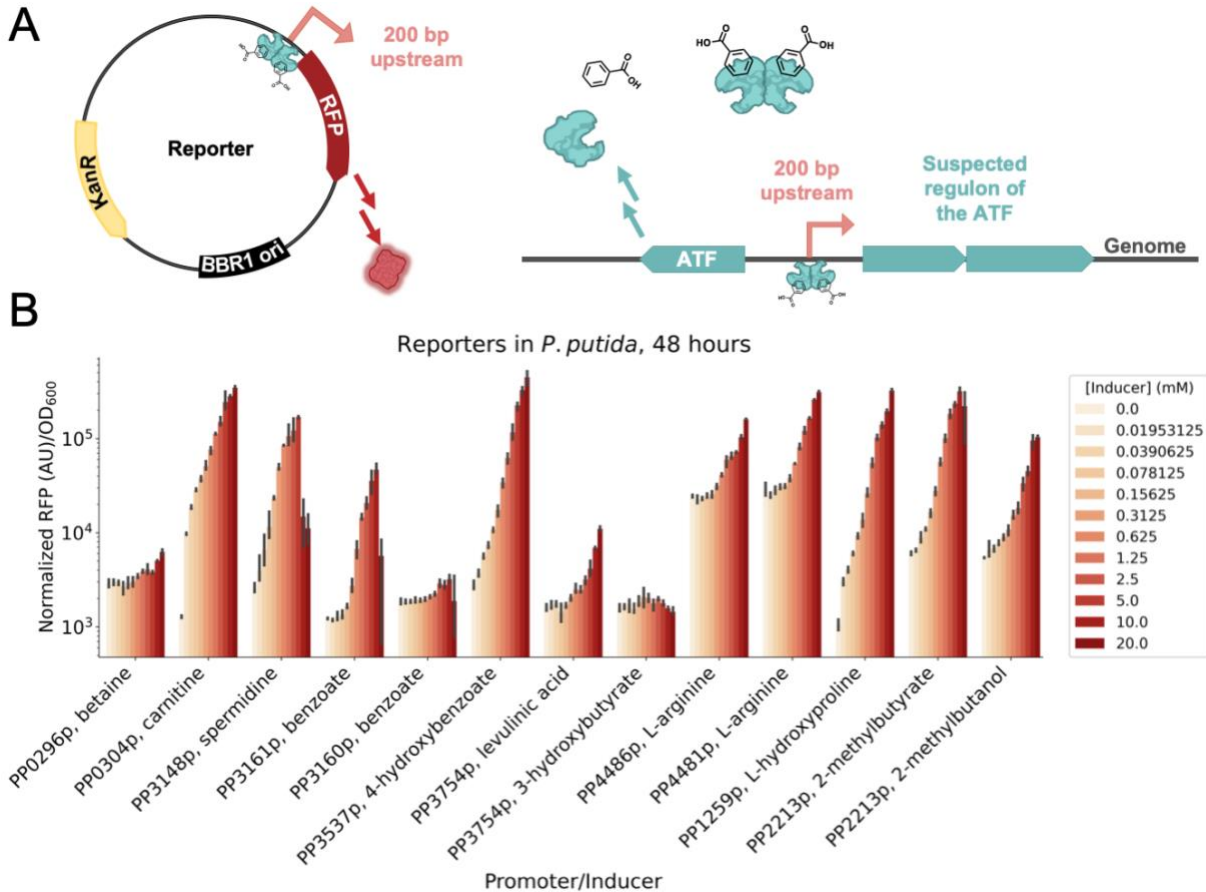
2

### 3 **Promoter characterization in *P. putida***

4 From the predicted regulon for the AFRs, we extracted the 200 base pairs upstream of  
5 the genes and constructed reporter plasmids with the promoters driving red fluorescent protein  
6 (RFP) expression. We then tested these reporter plasmids (plasmids pIP12-pIP23) in *P. putida*  
7 (strains sIP1-sIP12) for their response to the predicted ligand in minimal medium (Figure 2A)  
8 (Tables S1, S2). The predicted 3-hydroxybutyrate (P<sub>PP\_3754</sub>) and betaine (P<sub>PP\_0296</sub>) responsive  
9 promoters (sIP7, sIP1) both showed minimal induction in the corresponding test conditions.  
10 However, P<sub>PP\_3754</sub> (sIP7) did show a weak (6.9-fold induction) response to levulinic acid, which  
11 agrees with our RB-TnSeq data, indicating that the AFR/promoter pair PP\_3753/P<sub>PP\_3754</sub> might  
12 be involved in the regulation of levulinic acid or 3-hydroxypentanoyl-CoA catabolism.  
13 Interestingly, with maximum inductions of 6.5 and 11-fold, the two L-arginine responsive  
14 promoters (sIP8, sIP9) had similar dose dependent responses while sharing little homology in  
15 their nucleotide sequence. With 67-fold maximum induction at an inducer concentration of 5  
16 mM, P<sub>PP\_3148</sub> (sIP3) exhibited a moderate response to spermidine; however, the cells failed to  
17 reach a high OD at spermidine concentrations higher than 10 mM, likely due to toxicity from  
18 spermidine itself or a downstream metabolite. Similarly, the promoter P<sub>PP\_3161</sub> (sIP4) was  
19 induced 38-fold above background at 10 mM benzoate, but was hampered at 20 mM benzoate  
20 due to a presumed toxic effect on cell growth. Both 2-methylbutyrate and 2-methylbutanol  
21 induced moderate expression from the predicted promoter P<sub>PP\_2213</sub>, (sIP11) at 52 and 19-fold  
22 induction, respectively. P<sub>PP\_3537</sub> (sIP6) demonstrated a strong response to 4-hydroxybenzoate,  
23 with a maximum of 160-fold induction following supplementation with p-HB. Finally, the  
24 predicted carnitine (P<sub>PP\_0304</sub>) and L-hydroxyproline (L-HPro) (P<sub>PP\_1259</sub>) responsive promoters

1 (sIP2 and sIP12, respectively) both demonstrated high expression in the presence of their  
 2 respective inducers and tight repression, with 270 and 310 -fold induction (Table 1).

3



4

5 Figure 2. A) Schematic of the reporter plasmids used in *P. putida* to assay for inducibility. B)  
 6 Bar chart showing the induction of the promoter (x-axis) with their cognate inducer in *P. putida*  
 7 grown in minimal medium supplemented with 10 mM glucose. Promoters (200 bp upstream of  
 8 start codon) for each gene were induced with the predicted ligand. P<sub>PP\_0296</sub> (sIP1) with betaine,  
 9 P<sub>PP\_0304</sub> (sIP2) with carnitine, P<sub>PP\_3148</sub> (sIP3) with spermidine, P<sub>PP\_3161</sub> (sIP4) and P<sub>PP\_3160</sub> (sIP5)  
 10 with benzoate, P<sub>PP\_3537</sub> (sIP6) with para-hydroxybenzoate, P<sub>PP\_3754</sub> (sIP7) with 3-hydroxybutyrate  
 11 and levulinic acid, P<sub>PP\_4486</sub> (sIP8) and P<sub>PP\_4481</sub> (sIP9) with L-arginine, P<sub>PP\_1259</sub> (sIP12) with L-  
 12 hydroxyproline, and P<sub>PP\_2213</sub> (sIP11) with 2-methylbutyrate and 2-methylbutanol. (n=3, error  
 13 bars=95% confidence interval).

14

15

16

17

## 1 **Development of inducible systems in *E. coli***

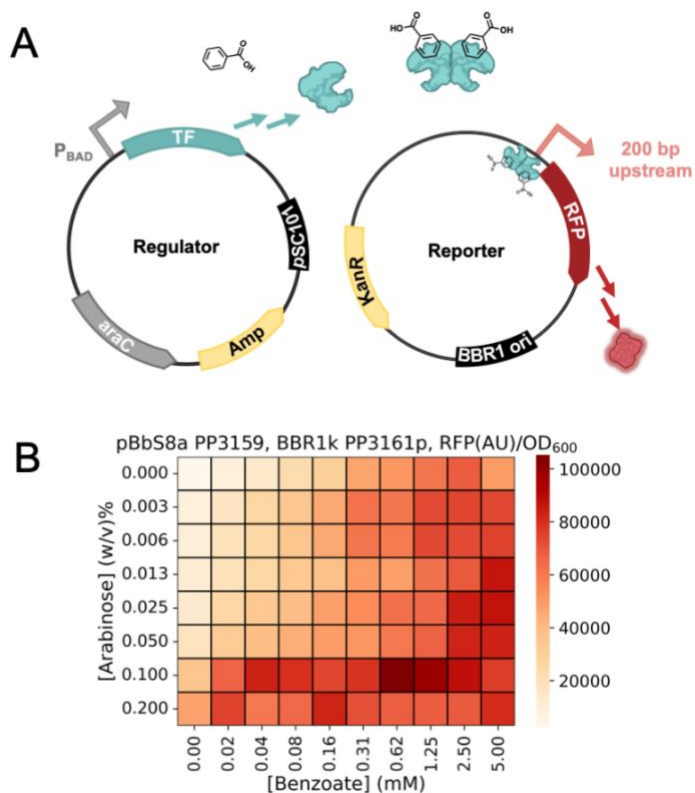
2           Following the promoter assay in *P. putida*, we next sought to validate the requirement for  
3 the corresponding AFRs via heterologous expression in *E. coli*. We used a previously described  
4 two-plasmid strategy, cloning the AFRs into arabinose-inducible ‘regulator’ vectors (plasmids  
5 pIP1-pIP9) and transforming them into *E. coli* carrying their cognate reporter plasmids (plasmids  
6 pIP12-pIP23) – the same constructs used to test the inducible activity of the promoters in *P.*  
7 *putida* (Figure 3A, Table S1)<sup>23</sup>. The resultant strains (strains sIP13-sIP24) allowed us to vary  
8 both the AFR expression level and inducer concentration in a high-throughput manner (Table  
9 S2).

10           We constructed a two-plasmid system using BenR as a test case. BenR is an AFR with  
11 a well-characterized response to benzoate in regulating the 69 base-pair *Pb* promoter<sup>29</sup>. In the  
12 two-plasmid system (sIP16), BenR is regulated by the canonical AraC- $P_{BAD}$  system (pIP4), and  
13 the region 200 bp upstream of PP\_3161 ( $P_{PP\_3161}$ ) was used as the promoter for RFP (pIP15)  
14 (Figure 3A). With the knowledge that this region contained the characterized *Pb* promoter, we  
15 expected induction of RFP to coincide with increasing concentrations of arabinose and  
16 benzoate<sup>26</sup>. Our results indicate that the promoter region was intact and that the expression of  
17 the regulator is titratable with arabinose (Figure 3B).

18           We tested the eight other inducible systems in the same manner as BenR.  
19 PP\_4482/ $P_{PP\_4481}$  (sIP21) and PP\_4482/ $P_{PP\_4486}$  (sIP20) had increased RFP expression with  
20 increased expression of the regulator. However, the induction of RFP did not seem to be  
21 affected by the addition of exogenous L-arginine (Figures S2I, S2J). Similarly, PP\_2211/ $P_{PP\_2213}$   
22 (sIP23) demonstrated a RFP response when the regulator was induced, but this response also  
23 did not increase when the putative inducers, 2-methylbutanol and 2-methylbutyrate, were added  
24 to the medium (Figure S2K, S2L). Likewise, PP\_3538/ $P_{PP\_3537}$  (sIP18) demonstrated a slight  
25 increase in RFP expression upon induction of the regulator, but there was no titratable response  
26 to the addition of 4-hydroxybenzoate, although this may be due to lack of transport across the



1 membrane (Figures S2F, S3). There was no clear correlation with inducer or regulator  
 2 expression to RFP expression in the cases of PP\_0298/P<sub>PP\_0296</sub> (sIP13), PP\_0305/P<sub>PP\_0304</sub>  
 3 (sIP14), PP\_3148/P<sub>PP\_3149</sub> (sIP15), or PP\_3754/P<sub>PP\_3753</sub> (sIP19) (Figure S2A, S2B, S2C, S2D,  
 4 S2E, S2G). There did appear to be a response to both inducer and regulator expression in the  
 5 instance of PP\_4602/P<sub>PP\_1259</sub> (sIP24), and this is further described in a later section.



6  
 7 Figure 3. A) Schematic of two-plasmid system used in *E. coli* to assay promoter-transcription  
 8 factor relationships. The transcription factor is induced on a low copy pSC101 plasmid with the  
 9 addition of arabinose, and the expression of RFP is driven by the cognate promoter for the  
 10 transcription factor B) Data from the two-plasmid system (sIP16) carrying the PP\_3161  
 11 promoter and inducible BenR (PP\_3159), n = 3. Plot of SD shown in Figure S1. Cells were  
 12 cultured in LB medium for 24 hours.

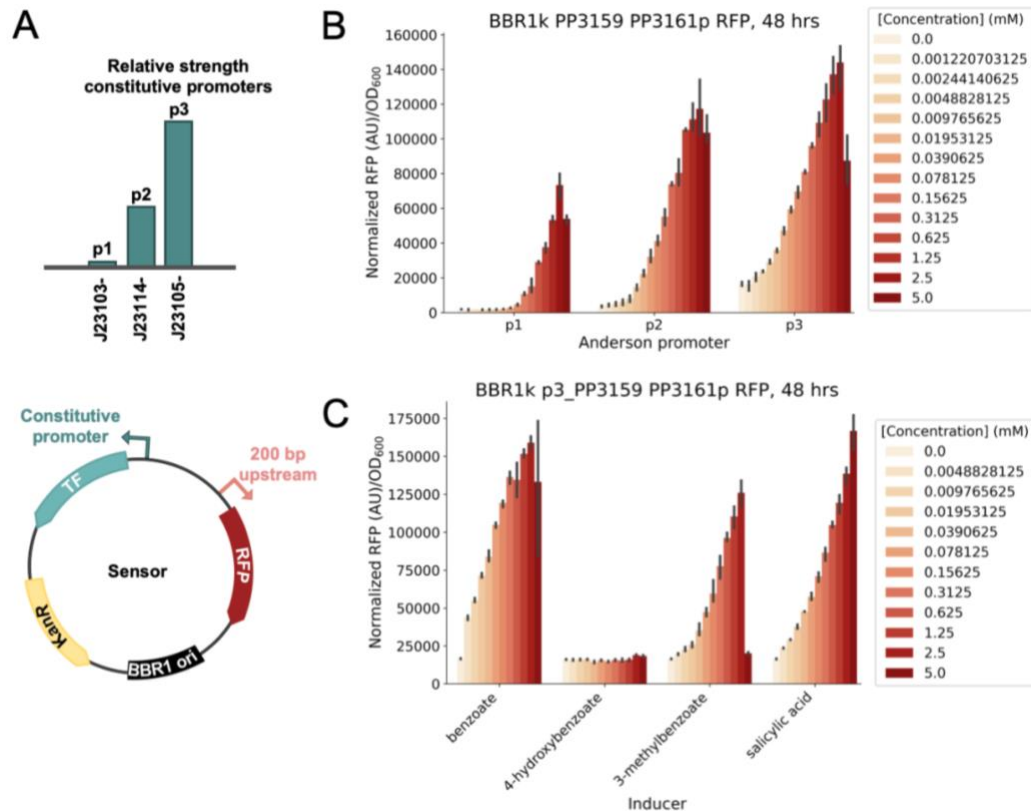
13

### 14 ***PP\_3159 (BenR) responds to multiple benzoates***

15 Following the success with the two-plasmid system, we developed three one-plasmid  
 16 systems (plasmids pIP33-pIP35) employing the benzoate-inducible BenR and also tested them  
 17 in *E. coli* (strains sIP39-sIP41)(Table S1, Table S2). Each one-plasmid system had a different

1 strength constitutive promoter driving the expression of *benR* and the 200 bp upstream of  
2 PP\_3161 controlling expression of RFP<sup>30</sup>. Each variant showed different sensor dynamics with  
3 the p1 variant (sIP39) having the tightest repression and  $38 \pm 3.9$  fold induction, the p3 variant  
4 (sIP41) showing the highest sensitivity and  $8.7 \pm 0.98$  -fold induction, and the p2 variant (sIP40)  
5 showing an intermediate level of sensitivity and repression with  $33 \pm 6.2$  -fold induction (Figures  
6 4A, 4B).

7 BenR has previously been described as a highly specific benzoate-responsive  
8 transcription factor<sup>29,31</sup>, but we found that it also responds to structurally similar compounds. We  
9 tested three functionalized benzoates with our one-plasmid system containing the strong p3  
10 promoter expressing *benR* (sIP41). Surprisingly, we found that our one-plasmid system  
11 responded to 3-methylbenzoate and salicylate in addition to benzoate (Figure 4C). The maximal  
12 induction by 3-methylbutyrate was ~ 80% of induction by benzoate, while the maximal induction  
13 by salicylate and benzoate were roughly the same. However, the system's response to  
14 benzoate was stronger than salicylate at low concentrations. This could be due to the inclusion  
15 of a secondary BenR binding site in our construct or because of high BenR expression from the  
16 p3 promoter, which is apparent in the high background fluorescence of this system (Figures 4A,  
17 4B).



1  
 2 Figure 4. Single plasmid system for BenR (n=3, error bars=95% confidence interval). A)  
 3 Schematic of the one-plasmid systems with constitutive promoters driving expression of the  
 4 transcription factor, and RFP under the control of the transcription factor. The bars (not to scale)  
 5 are labeled with the relative strength of the three Anderson promoters used. B) Dose  
 6 dependent response bar plots showing increasing benzoate concentrations induce expression  
 7 of RFP. C) Induction of RFP from the p3 single plasmid BenR system (sIP41) with  
 8 functionalized benzoates. Induction studies were conducted for 48 hours in LB medium.

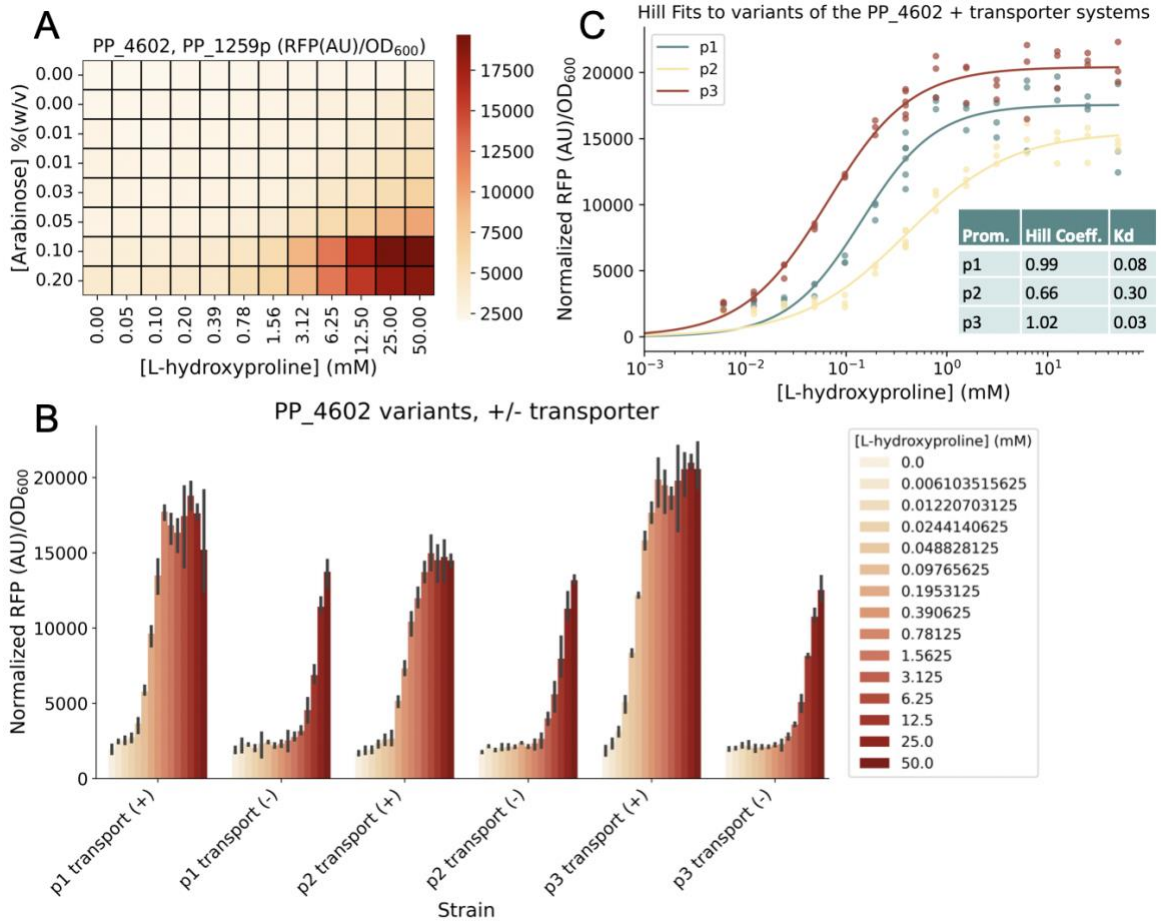
9

### 10 ***PP\_4602 allosteric response is enhanced with coexpression of a transporter***

11 The AFR PP\_4602 exhibited a specific phenotype ( $|t\text{-score}| > 4$ ,  $|\text{fitness}| > 1$ ) in the RB-  
 12 TnSeq data with trans-L-4-hydroxyproline (L-HPro) as the carbon source. The only other genes  
 13 displaying specific phenotypes in this condition are the predicted L-HPro assimilation genes  
 14 located at loci PP\_1255, PP\_1256, PP\_1257, PP\_1258, and PP\_1259. A unique characteristic  
 15 of PP\_4602 is that it lacks a typical AFR ligand binding domain, instead it contains a N-terminal  
 16 Per-Arnt-Sim (PAS) domain. This domain, as observed in other proteins, is involved in ligand  
 17 binding<sup>32,33</sup>. Homology and fitness data suggest that this AFR is expected to behave similarly to

1 LhpR (PA1261) from *Pseudomonas aeruginosa*, considering the significant sequence similarity  
2 (57% identity) of their ligand binding domains <sup>34</sup>.

3         In *P. putida*, P<sub>PP\_1259</sub> (sIP12) demonstrated a pronounced response to L-HPro, which  
4 makes it a promising candidate for the creation of an inducible system in *E. coli* (Figure 2B). The  
5 PP\_4602/P<sub>PP\_1259</sub> two-plasmid system (sIP24) exhibited a tunable response with the induction of  
6 the transcriptional regulator and the inclusion of the suitable inducer, L-HPro (Figure 5A, S4).  
7 Subsequently, we built three single-plasmid systems (plasmids pIP24-pIP26) and evaluated  
8 their response to L-HPro in *E. coli* (strains sIP30-sIP32) (Tables S1, S2). Although these  
9 inducible systems exhibited a clear response at an average of  $7.1 \pm 1.1$  fold induction, they did  
10 not attain maximal induction at the same concentration observed in *P. putida* (Figures 2B, 5B).  
11 After adding the predicted transporter, PP\_1259, to be co-transcribed with the ATF in the the  
12 single-plasmid system (pIP27-pIP29, sIP33-sIP35), maximal induction was reached at much  
13 lower L-HPro concentrations (390  $\mu$ M), the average fold induction across the three systems  
14 increased to  $9.8 \pm 2.6$ , and the systems conformed to the Hill equation (Figure 5C).



1

2 Figure 5. Systems for PP\_4602 (LhpR). A) Data from the two-plasmid system carrying the

3 PP\_1259 promoter and inducible lhpR (sIP24), n = 3. Plot of SD shown in Figure S4. B) Barplot

4 showing the inducibility of the PP\_4602 one-plasmid systems (sIP30-sIP35) with and without

5 the L-hydroxyproline transporter in a synthetic operon with lhpR (n=3, error bars=95%

6 confidence interval). C) Hill function fit to the PP\_4602 promoter variants with the L-

7 hydroxyproline transporter co-expressed with PP\_4602 (sIP33-sIP35). Cells were cultured in LB

8 medium for 24 hours.

9

### 10 **PP\_2211 putatively responds to 2-methylbutyryl-CoA**

11 The AFR PP\_2211 and the neighboring putative beta-oxidation system encoded by

12 PP\_2213-PP\_2217 have significant fitness defects ( $|t\text{-score}| > 4$ , fitness < 1) in the presence of

13 2-methylbutanol, L-isoleucine, and DL-2-aminobutyrate, indicating that these genes are

14 essential for the utilization of these compounds (Figure 1).<sup>14</sup> In *P. putida*, all three of these

15 compounds may share 2-methylbutyryl-CoA as a catabolic intermediate. Previous research has

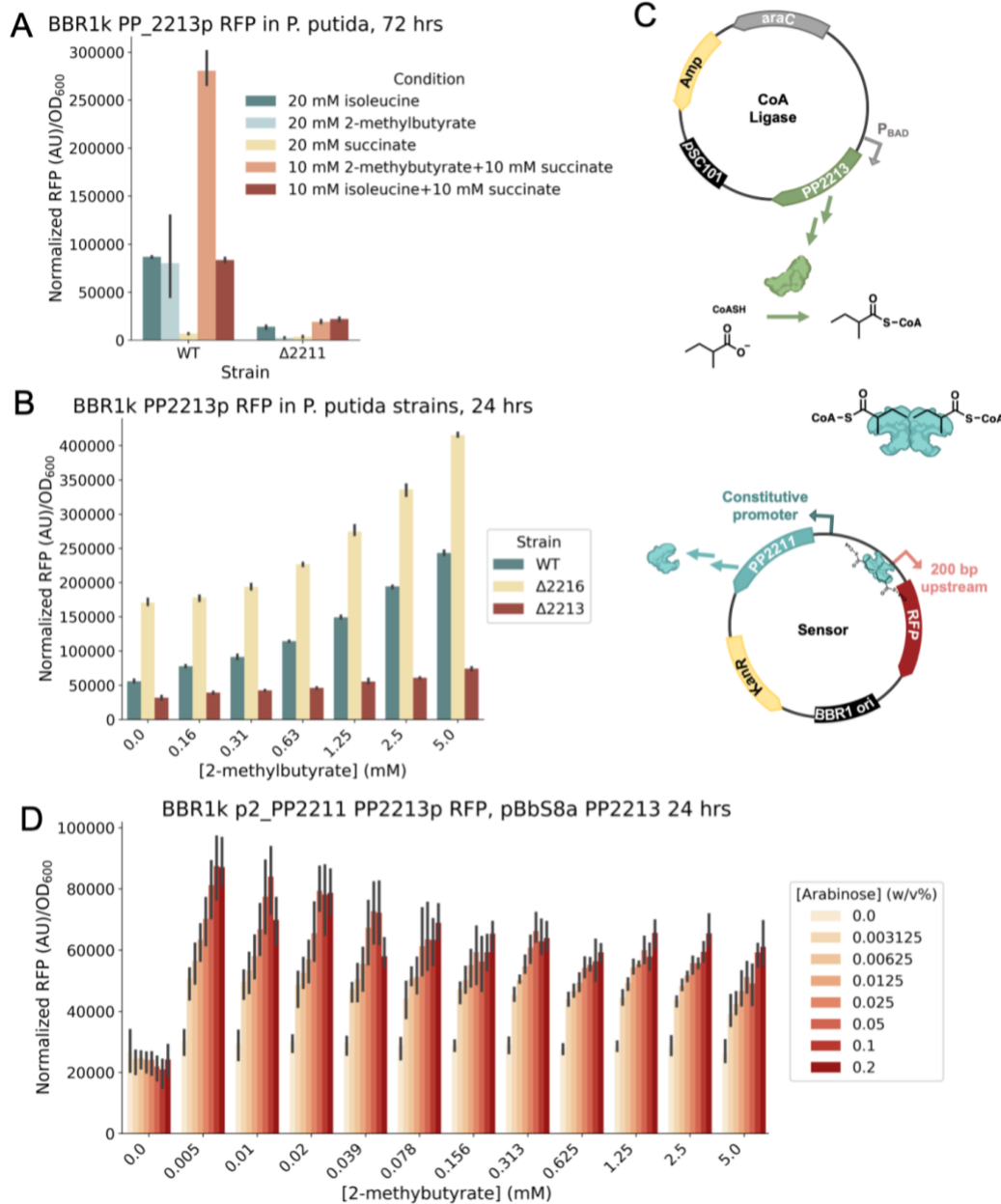
1 proposed that 2-methylbutanol is oxidized to 2-methylbutyrate, which subsequently undergoes  
2 beta-oxidation via the PP\_2213-PP\_2217 operon<sup>12</sup>. It has also been posited that 2-  
3 aminobutyrate is catabolized through deamination to 2-oxobutyrate, which is then funneled into  
4 L-isoleucine biosynthesis and subsequent catabolism<sup>14</sup>. The acyl thioester 2-methylbutyryl-CoA  
5 is a known intermediate during the catabolism of L-isoleucine.<sup>35</sup>

6 This suggests that PP\_2211 responds to free 2-methylbutyrate, 2-methylbutyryl-CoA, or  
7 a downstream metabolite. If the AFR PP\_2211 responds to free 2-methylbutyrate, then the  
8 fitness data would suggest that some thioesterase acts upon the 2-methylbutyryl-CoA produced  
9 during growth on isoleucine and 2-aminobutyrate. It is also possible that PP\_2211 may respond  
10 to 2-methylbutyryl-CoA itself or a downstream metabolite. To further examine this, we grew *P.*  
11 *putida* WT and  $\Delta$ PP\_2211 carrying the P<sub>PP\_2213</sub> reporter plasmid (sIP11, sIP27) with L-  
12 isoleucine, 2-methylbutyrate, and succinate as carbon sources in minimal medium (Figure 6A,  
13 Table S2). There was very little RFP expression in the  $\Delta$ PP\_2211 strain (sIP27), confirming that  
14 PP\_2211 regulates expression from P<sub>PP\_2213</sub>. The WT strain (sIP11) showed no significant RFP  
15 expression when strains were grown on succinate, moderate RFP expression when grown on L-  
16 isoleucine, 2-methylbutyrate, and isoleucine + succinate, and high RFP expression when grown  
17 on 2-methylbutyrate + succinate. If PP\_2211 responded to free 2-methylbutyrate, we would  
18 expect that the RFP expression levels would correlate directly to the amount of 2-methylbutyrate  
19 provided, but instead we see a dependence on succinate.

20 PP\_2211 may form a positive feedback loop with PP\_2213, which encodes a CoA ligase  
21 that also has a strong fitness phenotype and has been proposed to act on 2-methylbutyrate  
22 during 2-methylbutanol metabolism<sup>12</sup>. It is possible that this operon is a positive feedback loop,  
23 similar to the LacI system in *E. coli*<sup>36</sup>. PP\_2211 may respond to small amounts of a  
24 downstream product, such as 2-methylbutyryl-CoA, and upregulate expression of the PP\_2213-  
25 PP\_2217 operon. To test this hypothesis, we created a  $\Delta$ PP\_2213 strain and compared the  
26 response of the reporter plasmid to 2-methylbutyrate in this background (sIP28) versus the wild-

1 type background (sIP11). Maximal RFP expression was ~70% lower in the  $\Delta$ PP\_2213  
2 background (sIP28), indicating that PP\_2211 is likely responding to a downstream metabolite  
3 such as 2-methylbutyryl-CoA (Figure 6B). PP\_2216 is an acyl-CoA dehydrogenase posited to  
4 act on 2-methylbutyryl-CoA, and when we tested the reporter in a  $\Delta$ PP\_2216 strain (sIP29), we  
5 saw a ~70% increase in maximal RFP response (Figure 6B)<sup>12</sup>. This strongly suggests that  
6 PP\_2211 detects 2-methylbutyryl-CoA itself.

7 Finally, we sought to further probe this system in *E. coli* via a two-plasmid system. We  
8 created a strain (sIP25) that carried both a single-plasmid sensor variant (pIP30) and a plasmid  
9 with the CoA-ligase PP\_2213 (pIP10) under the control of the P<sub>BAD</sub> system (Figure 6D, Tables  
10 S1,S2). We varied the abundance of both the metabolite and the CoA-ligase PP\_2213 by  
11 growing this strain (sIP25) with different concentrations of 2-methylbutyrate and arabinose. We  
12 found that when expression of the CoA-ligase PP\_2213 was increased via the addition of  
13 arabinose, RFP expression from the sensor increased up to  $2.9 \pm 0.51$  -fold (Figure 6E). There  
14 was no RFP expression above background when no 2-methylbutyrate was added; however,  
15 beyond the lowest concentration of 2-methylbutyrate added (9.8  $\mu$ M), adding more 2-  
16 methylbutyrate did not increase the sensor response. Production of 2-methylbutyryl-CoA could  
17 be dependent on the amount of enzyme and not the amount of substrate due to feedback  
18 inhibition. 2-Methylbutyryl-CoA may allosterically inhibit the CoA ligase, similar to the  
19 *Rhodopseudomonas palustris* benzoate-CoA ligase<sup>37</sup>. Together, these data indicate that  
20 PP\_2211 responds to 2-methylbutyryl-CoA. We propose this AFR be named the 2-  
21 methylbutyrate regulator, TmbR.



1

2 Figure 6. Investigation of the PP\_2211/P<sub>PP\_2213</sub> system (n=3, error bars=95% confidence  
3 interval). A) Induction of RFP expression from P<sub>PP\_2213</sub> in *P. putida* WT (sIP11) and ΔPP\_2211  
4 (sIP27) background. Cultures were grown in MOPS minimal medium for 72 hours with the  
5 indicated carbon sources. B) Induction of RFP expression from P<sub>PP\_2213</sub> in *P. putida* under varied  
6 concentrations of 2-methylbutyrate in the *P. putida* WT (sIP11), ΔPP\_2216 (sIP29), and  
7 ΔPP\_2213 (sIP28) backgrounds. Cultures were grown in LB medium for 24 hours. C)  
8 Schematic of a two plasmid system used to characterize the P<sub>PP\_2213</sub> in *E. coli*. The CoA ligase  
9 plasmid features PP\_2213 expressed by the AraC-P<sub>BAD</sub> system (pIP10), while the sensor  
10 plasmid contains the PP\_2211/P<sub>PP\_2213</sub> system (pIP30). D) RFP expression from the system  
11 shown in part C. Cultures were grown in EZ Rich defined medium for 24 hours, supplemented  
12 with varying concentrations of arabinose and 2-methylbutyrate.  
13



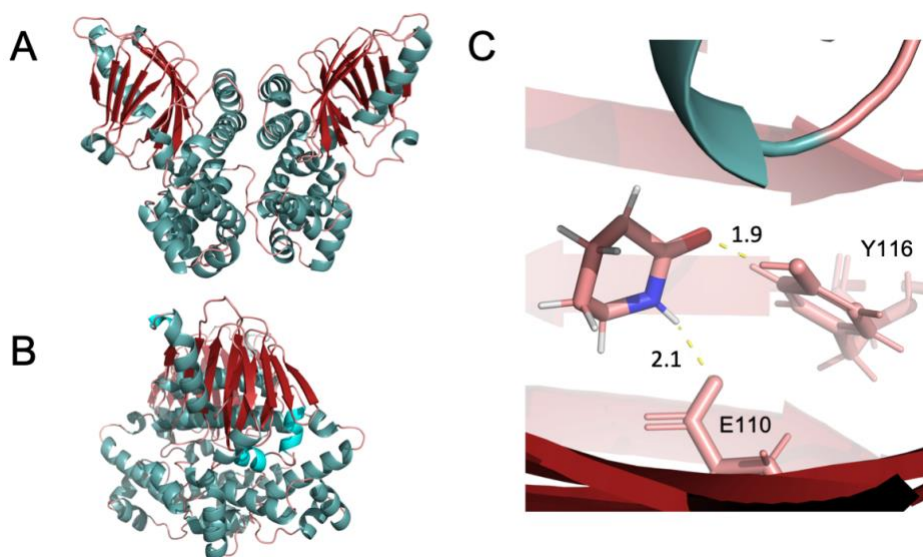
## 1 ***Rational mutations for altered ligand specificities***

2           Following development of the inducible systems for *E. coli*, we sought to alter the  
3 substrate specificity of the regulators via targeted mutagenesis. Using our local implementation  
4 of AlphaFold2, LBL Foldy, we predicted the protein structures for the AFRs investigated in this  
5 work <sup>16,38–40</sup> (Table S3). We noted PP\_3516 (OplR), PP\_4602 (LhpR), and PP\_3159 (BenR)  
6 contained pockets larger than a water molecule in their predicted ligand binding domains. Using  
7 *in silico* docking either with Autodock Vina or SwissDock <sup>41,42</sup>, we then docked the ligands to the  
8 structures (Figures 7, S5A, S6A). Following these predictions we generated rational mutations  
9 in PP\_4602, BenR, and OplR to alter their ligand specificity.

10           The AFR PP\_4602 was annotated as having a non-canonical start site TTG, and the  
11 naive AlphaFold structure prediction shows that the first 20 amino acids encode a disordered,  
12 low predicted accuracy alpha helix. Upon further interrogation, we identified an internal  
13 methionine with a canonical ATG start codon 20 amino acids into the annotated sequence. We  
14 chose this as the start site for the rest of our *in silico* analyses. The signal sensing domain of  
15 PP\_4602 is smaller than the other AFRs in this study while still containing a distinct cavity within  
16 it, but this cavity was not large enough to accommodate L-HPro. Following *in silico* repacking  
17 via sidechain and backbone energy minimization in FoldIt-Standalone, the pocket could  
18 accommodate L-HPro, and ligand binding was predicted with SwissDock (Table S3) <sup>41–44</sup>.

19           With this new prediction, we identified four residues with possible H-bond interactions  
20 with the ligand. In one predicted binding mode, K46 and K123 appear to be H-bonding with the  
21 carboxylic acid group of L-HPro. R62 was within H-bonding distance to the hydroxyl, and Y52  
22 was near the secondary amine (Figure S5A). With this information, we predicted a mutation in  
23 K46 or K123 into an H-bond acceptor like glutamate or aspartate could confer a response to S-  
24 or R-4-hydroxy-2-pyrrolidinone (S or R-HPyr). However, following individual mutations at K46  
25 and K123 (plasmids pIP40-pIP41), the sensor did not respond to S/R-HPyr or L-HPro in *E. coli*  
26 (strains sIP46-sIP47) (Figure S5B, TableS1-S2).

1 We hypothesized mutations in BenR could also enable a response to benzyl-alcohol and  
2 benzaldehyde. H32 appeared to form pi-stacking while Y61 and Y115 made H-bonds with the  
3 benzoate ligand docked to the structure (Figure S6A). We mutated residues H32A, Y61F, and  
4 Y115F (pIP37-pIP39) in an attempt to yield a transcription activation response to benzyl alcohol  
5 and benzaldehyde in *E. coli* (sIP43-sIP45). These mutations also abolished all inducible activity  
6 (Figure S6B and C). However, our characterization of both the LhpR and BenR mutants  
7 indicated that the residues we chose may be essential for signal transduction or ligand binding .  
8



9  
10 Figure 7. AlphaFold-predicted structure of OpIR. A) 'Front' view of OpIR structure. B) OpIR  
11 structure rotated 90 degrees along the vertical axis. C) Zoomed in view of OpIR ligand binding  
12 site docked with valerolactam via AutoDock Vina showing E110 and Y116 with hydrogen bonds  
13 depicted to the valerolactam ligand. Distances are in angstroms.

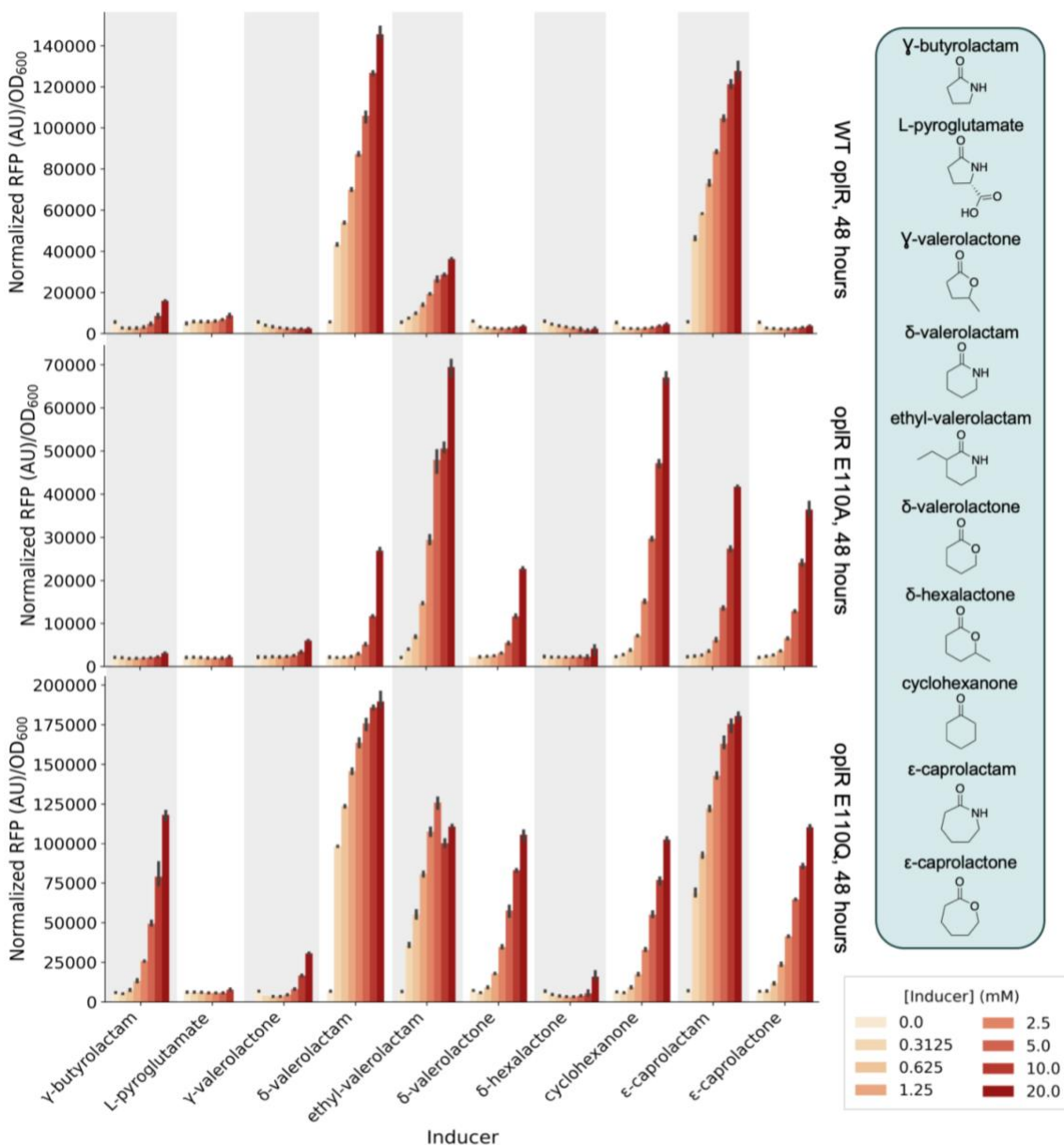
14  
15 Finally, we chose the caprolactam and valerolactam responsive ATF, OpIR, as our final  
16 test case for mutational analysis, and successfully changed its substrate specificity<sup>23</sup>. We  
17 identified the residues defining the ligand binding pocket of OpIR and found six residues with  
18 polar groups. It appeared that Y116 and E110 could form H-bonds with the oxygen and nitrogen  
19 of the amide, respectively. We hypothesized that a mutation at E110 to an H-bond donor such

1 as glutamine would confer a response to valerolactone and caprolactone. E110Q (pIP43, sIP49)  
2 resulted in inducible expression by both valero- and capro- lactam and lactone (Figure 8, Table  
3 2). Surprisingly, we also found the E110Q mutation enabled a response to many more cyclic  
4 ligands (Figure 8, Table 2). Furthermore, an alanine-substituted mutant, E110A (pIP42, sIP48),  
5 was more selective in ligand specificity, favoring cyclohexanone and ethyl-valerolactam. OpIR  
6 E110A (sIP48) also exhibited approximately 60% lower background fluorescence than wildtype  
7 and 70% lower background than E110Q (sIP49), while exhibiting the highest -fold induction ( $33$   
8  $\pm 1.2$ , for ethyl-valerolactam) out of the tested OpIR variants (Figure 8, Table 2).

9

10 Table 2. OpIR WT and mutants with their response to tested lactam and lactone inducers. The  
11 fold induction values shown are between the maximum measured normalized RFP values and  
12 the uninduced controls. Fold induction values  $<1$  are indicated by NI (no induction).  $n = 3$ , error  
13 = standard deviation.

Tested inducer	Fold induction of WT OpIR	Fold induction of OpIR E110A	Fold induction of OpIR E110Q
$\gamma$ -butyrolactam	$2.8 \pm 0.10$	$1.5 \pm 0.05$	$20 \pm 1.0$
L-pyroglutamate	$1.8 \pm 0.17$	$1.0 \pm 0.09$	$1.2 \pm 0.07$
$\gamma$ -valerolactone	NI	$2.8 \pm 0.16$	$4.5 \pm 0.05$
$\delta$ -valerolactam	$25 \pm 0.62$	$12 \pm 0.6$	$28 \pm 0.9$
ethyl-valerolactam	$6.5 \pm 0.20$	$33 \pm 1.2$	$19 \pm 0.8$
$\delta$ -valerolactone	NI	$10 \pm 0.1$	$14 \pm 0.5$
$\delta$ -hexalactone	NI	$1.8 \pm 0.49$	$2.3 \pm 0.42$
cyclohexanone	NI	$30 \pm 0.9$	$16 \pm 0.3$
$\epsilon$ -caprolactam	$22 \pm 0.8$	$18 \pm 0.5$	$25 \pm 0.7$
$\epsilon$ -caprolactone	NI	$17 \pm 0.8$	$16 \pm 0.2$



1

2 Figure 8. Response of OpIR wild-type and mutant variants (sIP48-sIP49) in *E. coli* to ten cyclic  
 3 inducers:  $\gamma$ -butyrolactam, L-pyroglutamate,  $\gamma$ -valerolactone,  $\delta$ -valerolactam, ethyl-valerolactam,  
 4  $\delta$ -valerolactone,  $\delta$ -hexalactone, cyclohexanone,  $\epsilon$ -caprolactam, and  $\epsilon$ -caprolactone. The  
 5 mutants and WT demonstrate different substrate specificities. Cultures were grown in LB  
 6 medium with each inducer for 48 hours (n=3, error bars=95% confidence interval).

7

## 8 Discussion:

9 Here we have described a process for identifying and characterizing transcription factors

10 using public data derived from the high throughput functional genomics method, RB-TnSeq, and

1 its application to the AraC-family transcription factors in *P. putida*. We first employed RB-TnSeq  
2 data to hypothesize AFR-promoter-inducer pairings. Then we reintroduced these promoter  
3 regions into the native host (*Pseudomonas putida* KT2440) as reporter systems (sIP1-sIP12)  
4 and observed whether they enabled titratable gene expression in the presence of the suspected  
5 inducer. With functional knockouts in downstream genes, this series of reporters could be  
6 employed in *P. putida* for bioengineering or general microbiology studies. We next developed a  
7 series of inducible plasmids (pIP24-pIP35) that enable expression with diverse inducers in *E.*  
8 *coli* (sIP30-sIP41). These systems can further be employed in a manner akin to the canonical  
9 P<sub>BAD</sub> inducible system. Finally, we demonstrated how protein structure predictions via  
10 AlphaFold2 and FoldIt can be further used to gain a deeper understanding of these proteins  
11 through targeted mutations either resulting in disrupted induction activity or in modulated  
12 activity, further expanding the diversity of these regulators.

13         Interestingly, PP\_4602 shows homology to the regulator of the L-HPro degradation  
14 system in *P. aeruginosa*, LhpR, but it is distal from the other genes involved in L-HPro  
15 degradation<sup>34</sup>. This regulator and its promoter are located near identical predicted transposable  
16 elements. This may indicate that the regulator migrated via a spurious transposition or  
17 recombination event. The inducible systems (pIP24-pIP26) developed from this regulator show  
18 both low background in rich medium and high induction in the presence of L-HPro when tested  
19 in *E. coli* (sIP30-sIP32). Incorporating the L-HPro transporter from *P. putida* into the one-  
20 plasmid systems (pIP27-pIP29) resulted in peak induction at lower concentrations of HPro in *E.*  
21 *coli* (sIP33-sIP35) (Figure 5A). However, in all tested constructs, the use of constitutive  
22 promoters with different strengths to drive expression of the ATF did not appear to have a  
23 significant effect on sensor dynamics. Our AlphaFold2 structure predictions indicated that the  
24 true start codon might be 60 bp downstream of the currently annotated start codon, which could  
25 explain this observation.

1           The benzoate catabolism regulator, BenR (PP\_3159) is proximal to a hypothetical  
2 protein, PP\_3160. After testing this gene's promoter in *P. putida*, we showed that it is not  
3 responsive to benzoate, unlike the promoter region 5' of PP\_3161 (*Pb*). The exact function of  
4 PP\_3160 is still unknown. The three BenR-derived single-plasmid systems (pIP33-pIP45) we  
5 developed have different sensitivities and dynamic ranges in *E. coli* (sIP39-sIP41) and could be  
6 employed as expression systems for metabolic engineering applications. We found that our p3  
7 single-plasmid construct (sIP41) was strongly induced by 3-methylbenzoate and salicylate, in  
8 addition to benzoate. This differs from previously described reports that BenR demonstrates  
9 little to no response to these molecules<sup>31</sup>. We did use a longer sequence as the 'promoter'  
10 region than in previous work; our 200 base-pair 'promoter' for RFP expression contains the  
11 canonical 69 base-pair *Pb* promoter as well as a portion of the upstream gene, PP\_3160, and it  
12 is possible that our constructs included a secondary BenR binding site<sup>26</sup>. Previous work has  
13 found that adding an additional BenR binding site to the *Pb* promoter enabled a weak response  
14 to 3-methylbenzoate.<sup>29</sup> Another explanation could be that our constructs yielded higher  
15 intracellular concentrations of BenR than are present natively, amplifying the effect of weak  
16 binding to these 3-methylbenzoate and salicylate. The use of constitutive promoters driving  
17 expression of the transcription factor may be useful in identifying weak activities to inducers and  
18 guide protein engineering efforts.

19           From 2-methylbutanol, L-isoleucine, and 2-aminobutyrate RB-TnSeq data, we identified  
20 an AFR (PP\_2211, TmbR) with a potentially novel ligand specificity for 2-methylbutyryl-CoA.  
21 This would be a novel ligand specificity for AFRs, as no prior AFR has been described to have a  
22 response to an acyl-CoA, and TmbR may be applicable as a biosensor for pathways relying on  
23 these molecules. While we could not identify a discreet ligand binding pocket for this protein  
24 based on AlphaFold structural predictions, directed evolution methods could be conducted to  
25 enhance the response to 2-methylbutyryl-CoA or enable a response to another acyl-CoA of  
26 interest.

1           Finally, we successfully leveraged an AlphaFold structure to make informed mutations  
2 and change the substrate specificity of the characterized valerolactam responsive transcription  
3 factor, OplR<sup>16,38,45</sup>. AutoDock Vina resolved a potential binding mode for valerolactam in the  
4 predicted ligand binding domain of OplR<sup>39,40</sup>. A single mutation, E110A, in this site enabled  
5 broader substrate specificity and responses to ligands which had no inducible activity in the  
6 wildtype protein and reduced the inducible response to valerolactam (Figure 8). We  
7 hypothesized that another mutation, E110Q, would enable an allosteric response to lactones.  
8 Not only did the E110Q mutant (sIP49) respond to valerolactone and caprolactone, it also  
9 responded to cyclohexanone, enhanced the response to ethyl-valerolactam and butyrolactam,  
10 and provided a weak response to gamma-valerolactone (Table 2). These constructs could prove  
11 to be a starting point for further mutation of OplR and diversification of its inducer space.  
12 Lactams, lactones, and their derivatives are targets for bioproduction, and increasing the range  
13 of these compounds that genetically-encoded biosensors can detect may aid in future  
14 engineering efforts<sup>46,47</sup>.

15           The identification of these regulators enabled the rapid development of transcription  
16 factor-based inducible systems that can be used in all fields requiring engineered protein/RNA  
17 expression. The systems derived from the benzoate and L-HPro responsive ATFs/promoters  
18 (PP\_3159/P<sub>PP3161</sub>, PP\_4602/P<sub>PP1259</sub>) were functional in both *P. putida* and *E. coli*. Experiments in  
19 both organisms also indicated that PP\_2211 (TmbR) likely responds to 2-methylbutyryl-CoA, a  
20 novel inducer type for an ATF. Finally, we created targeted mutations in the AFR OplR that  
21 altered its inducer specificity.

22           We have explored the AraC family of transcription factors in *P. putida* using public RB-  
23 TnSeq data, reporter assays, inducible systems, and AlphaFold2. The approach utilized in this  
24 work could be used to study additional transcription factor families in *P. putida* or other  
25 organisms. Such characterization of transcription factors expands our fundamental biological  
26 knowledge and our tools for metabolic engineering and synthetic biology.

1

## 2 **Methods:**

### 3 ***Plasmids and Strains***

4 The bacterial strains and plasmids utilized in this research are detailed in Tables S1 and S2.  
5 Any strains and plasmids generated during this research are accessible via the public JBEI  
6 registry. (<https://public-registry.jbei.org/folders/792>). We designed all plasmids through the  
7 Device Editor and Vector Editor software, and j5 software was used for designing all primers  
8 that were involved in the plasmid construction process<sup>48–50</sup>. We assembled the plasmids  
9 through Gibson Assembly following standard procedures<sup>51</sup>. Routine isolation of the plasmids  
10 was performed using the Qiaprep Spin Miniprep kit from Qiagen, USA, while all primers were  
11 procured from Integrated DNA Technologies (IDT, Coralville, IA). DNA sequencing was  
12 conducted through Primordium (Monrovia, CA)

13

### 14 ***Chemicals, media, growth conditions***

15 *E. coli* and *P. putida* were cultivated in Lysogeny Broth (LB) Miller medium (sourced from BD  
16 Biosciences, USA) at a temperature of 37°C and 30°C, respectively. When necessary, strains  
17 were also cultured in EZ-Rich medium (obtained from Teknova, Hollister, CA) with a 10 mM  
18 glucose supplement. Minimal media experiments were conducted with MOPs buffered minimal  
19 medium prepared according to LaBauve et al<sup>52</sup>. As needed, the cultures were enriched with  
20 kanamycin (50 mg/L from Sigma-Aldrich, USA), carbenicillin (100 mg/L from Sigma-Aldrich,  
21 USA) or gentamicin (30 mg/L from Sigma-Aldrich, USA). All additional chemicals were acquired  
22 from Sigma-Aldrich (Sigma-Aldrich, USA).

23

### 24 ***Fluorescence assays***

25 Endpoint assays were carried out in 96-deep well plates (procured from Corning Costar, model  
26 3960). Each well was filled with 500 µL of a medium that included necessary ligands, antibiotics,



1 and/or inducers, with an inoculation of 1% v/v sourced from overnight cultures. These plates  
2 were sealed with an AeraSeal film (from Excel Scientific, model AC1201-02) and incubated at  
3 30°C or 37°C on a 250 rpm shaker rack. After 24 and/or 48 hours where specified, 100 µL from  
4 every well was distributed into a black, clear-bottom 96-well plate (Corning Costar, 3603) to  
5 measure optical density and fluorescence using an Biotek Synergy H1 (Agilent, Santa Clara,  
6 CA) plate reader. Optical density was evaluated at 600 nm (OD<sub>600</sub>), and fluorescence was  
7 assessed using an excitation wavelength of 535 nm, an emission wavelength of 620 nm, and a  
8 manually set gain of 100.

9

### 10 **Structure predictions and docking**

11 Structure predictions were conducted with the Foldy implementation of AlphaFold2<sup>38,45</sup>. All  
12 AFRs were folded as monomers and dimers and were docked to the predicted ligand based on  
13 the RB-TnSeq datasets. Docking was conducted in the Foldy UI using AutoDock Vina as the  
14 docking algorithm<sup>39,40</sup>. For LhpR (PP\_4602), the protein structure prediction for the dimer was  
15 repacked using Foldit-Standalone, and docking was conducted using SwissDock<sup>41,43,44</sup>. No  
16 boundaries for ligand binding were specified in any of the docking experiments. Folds for all  
17 AFRs and dimers are available as public structures in the LBL implementation of Foldy, at  
18 <https://foldy.lbl.gov/> with the tag “AraC” (Table S1).

19

### 20 **Gene knockouts in *Pseudomonas putida***

21 Gene knockouts in *Pseudomonas putida* were made as previously described<sup>12</sup>. The allelic  
22 exchange vector pMQ30 was used for homologous recombination with *sacB* counterselection.  
23 Homology arms of roughly 1000 bp each, including the start and stop codons, were cloned into  
24 the pMQ30 vector. These vectors were then electroporated into *E. coli* S17 and subsequently  
25 conjugated into *P. putida*. Transconjugants were selected for on Pseudomonas isolation agar  
26 (Difco) supplemented with 30 mg/mL gentamicin. Putative knockouts were selected for on LB

1 plates with no NaCl and 10% w/v sucrose and screened via PCR with primers flanking the  
2 target gene.

3

#### 4 ***RB-TnSeq datasets and AFR identification***

5 RB-TnSeq data were collected from the fitness browser ([fit.genomics.lbl.gov](http://fit.genomics.lbl.gov)). These data  
6 included experiments from numerous publications, including data from the original paper  
7 describing the library <sup>11,12,14,22,53,54</sup>. AFRs were identified from the datasets by setting a t-score  
8 cutoff of  $\pm 4$  and screening for proteins containing the Pfam HTH\_18 (AraC family helix-turn-  
9 helix) domain <sup>21</sup>.

10

#### 11 **Acknowledgements:**

12 We thank Bridget Luckie and Peter Winegar for providing feedback on figure designs, and  
13 Michael Cronce, Isaac Donnell, and Aidan Cowan for sharing essential materials with us during  
14 the supply chain shortage. This work was part of the DOE Joint BioEnergy Institute  
15 (<https://www.jbei.org>) supported by the U.S. Department of Energy, Office of Science, Office of  
16 Biological and Environmental Research, supported by the U.S. Department of Energy, Energy  
17 Efficiency and Renewable Energy, Bioenergy Technologies Office, through contract DE-AC02-  
18 05CH11231 between Lawrence Berkeley National Laboratory and the U.S. Department of  
19 Energy. A.A.N. was supported by a National Science Foundation Graduate Research  
20 Fellowship, fellow ID [2018253421]. The views and opinions of the authors expressed herein do  
21 not necessarily state or reflect those of the United States Government or any agency thereof.  
22 Neither the United States Government nor any agency thereof, nor any of their employees,  
23 makes any warranty, expressed or implied, or assumes any legal liability or responsibility for the  
24 accuracy, completeness, or usefulness of any information, apparatus, product, or process  
25 disclosed, or represents that its use would not infringe privately owned rights. The United States  
26 Government retains and the publisher, by accepting the article for publication, acknowledges

1 that the United States Government retains a nonexclusive, paid-up, irrevocable, worldwide  
2 license to publish or reproduce the published form of this manuscript, or allow others to do so,  
3 for United States Government purposes. The Department of Energy will provide public access  
4 to these results of federally sponsored research in accordance with the DOE Public Access Plan  
5 (<http://energy.gov/downloads/doe-public-access-plan>).

6

## 7 **Competing Interests**

8 J.D.K. has financial interests in Amyris, Ansa Biotechnologies, Apertor Pharma, Berkeley Yeast,  
9 Demetrix, Lygos, Napigen, ResVita Bio, and Zero Acre Farms.

10

11

12

13

14

15

16

17

18

19

20

21

22

23

24

25

26

27

28

29

## 1 Bibliography

- 2 (1) Taylor, N. D., Garruss, A. S., Moretti, R., Chan, S., Arbing, M. A., Cascio, D., Rogers, J. K.,  
3 Isaacs, F. J., Kosuri, S., Baker, D., Fields, S., Church, G. M., and Raman, S. (2016) Engineering  
4 an allosteric transcription factor to respond to new ligands. *Nat. Methods* 13, 177–183.
- 5 (2) Rottinghaus, A. G., Xi, C., Amrofell, M. B., Yi, H., and Moon, T. S. (2022) Engineering ligand-  
6 specific biosensors for aromatic amino acids and neurochemicals. *Cell Syst.* 13, 204-214.e4.
- 7 (3) Reed, B., Blazeck, J., and Alper, H. (2012) Evolution of an alkane-inducible biosensor for  
8 increased responsiveness to short-chain alkanes. *J. Biotechnol.* 158, 75–79.
- 9 (4) Mitchler, M. M., Garcia, J. M., Montero, N. E., and Williams, G. J. (2021) Transcription factor-  
10 based biosensors: a molecular-guided approach for natural product engineering. *Curr. Opin.*  
11 *Biotechnol.* 69, 172–181.
- 12 (5) Schleif, R. (2010) AraC protein, regulation of the l-arabinose operon in Escherichia coli, and  
13 the light switch mechanism of AraC action. *FEMS Microbiol. Rev.* 34, 779–796.
- 14 (6) Bi, C., Su, P., Müller, J., Yeh, Y.-C., Chhabra, S. R., Beller, H. R., Singer, S. W., and Hillson,  
15 N. J. (2013) Development of a broad-host synthetic biology toolbox for *Ralstonia eutropha* and  
16 its application to engineering hydrocarbon biofuel production. *Microb. Cell Fact.* 12, 107.
- 17 (7) Romano, E., Baumschlager, A., Akmeriç, E. B., Palanisamy, N., Houmani, M., Schmidt, G.,  
18 Öztürk, M. A., Ernst, L., Khammash, M., and Di Ventura, B. (2021) Engineering AraC to make it  
19 responsive to light instead of arabinose. *Nat. Chem. Biol.* 17, 817–827.
- 20 (8) Guzman, L. M., Belin, D., Carson, M. J., and Beckwith, J. (1995) Tight regulation,  
21 modulation, and high-level expression by vectors containing the arabinose PBAD promoter. *J.*  
22 *Bacteriol.* 177, 4121–4130.
- 23 (9) Gawin, A., Valla, S., and Brautaset, T. (2017) The XylS/Pm regulator/promoter system and  
24 its use in fundamental studies of bacterial gene expression, recombinant protein production and  
25 metabolic engineering. *Microb. Biotechnol.* 10, 702–718.

- 1 (10) Gallegos, M. T., Schleif, R., Bairoch, A., Hofmann, K., and Ramos, J. L. (1997) Arac/XyIS  
2 family of transcriptional regulators. *Microbiol. Mol. Biol. Rev.* 61, 393–410.
- 3 (11) Thompson, M. G., Blake-Hedges, J. M., Cruz-Morales, P., Barajas, J. F., Curran, S. C.,  
4 Eiben, C. B., Harris, N. C., Benites, V. T., Gin, J. W., Sharpless, W. A., Twigg, F. F., Skyrud, W.,  
5 Krishna, R. N., Pereira, J. H., Baidoo, E. E. K., Petzold, C. J., Adams, P. D., Arkin, A. P.,  
6 Deutschbauer, A. M., and Keasling, J. D. (2019) Massively parallel fitness profiling reveals  
7 multiple novel enzymes in *Pseudomonas putida* lysine metabolism. *MBio* 10.
- 8 (12) Thompson, M. G., Incha, M. R., Pearson, A. N., Schmidt, M., Sharpless, W. A., Eiben, C.  
9 B., Cruz-Morales, P., Blake-Hedges, J. M., Liu, Y., Adams, C. A., Haushalter, R. W., Krishna, R.  
10 N., Lichtner, P., Blank, L. M., Mukhopadhyay, A., Deutschbauer, A. M., Shih, P. M., and  
11 Keasling, J. D. (2020) Fatty acid and alcohol metabolism in *Pseudomonas putida*: functional  
12 analysis using random barcode transposon sequencing. *Appl. Environ. Microbiol.* 86.
- 13 (13) Incha, M. R., Thompson, M. G., Blake-Hedges, J. M., Pearson, A. N., Schmidt, M.,  
14 Deutschbauer, A., and Keasling, J. D. (2019) Leveraging host metabolism for  
15 bisdemethoxycurcumin production in *Pseudomonas putida*. *BioRxiv*.
- 16 (14) Schmidt, M., Pearson, A. N., Incha, M. R., Thompson, M. G., Baidoo, E. E. K., Kakumanu,  
17 R., Mukhopadhyay, A., Shih, P. M., Deutschbauer, A. M., Blank, L. M., and Keasling, J. D.  
18 (2022) Nitrogen Metabolism in *Pseudomonas putida*: Functional Analysis Using Random  
19 Barcode Transposon Sequencing. *Appl. Environ. Microbiol.* 88, e0243021.
- 20 (15) Baek, M., DiMaio, F., Anishchenko, I., Dauparas, J., Ovchinnikov, S., Lee, G. R., Wang, J.,  
21 Cong, Q., Kinch, L. N., Schaeffer, R. D., Millán, C., Park, H., Adams, C., Glassman, C. R.,  
22 DeGiovanni, A., Pereira, J. H., Rodrigues, A. V., van Dijk, A. A., Ebrecht, A. C., Opperman, D.  
23 J., and Baker, D. (2021) Accurate prediction of protein structures and interactions using a three-  
24 track neural network. *Science* 373, 871–876.
- 25 (16) Jumper, J., Evans, R., Pritzel, A., Green, T., Figurnov, M., Ronneberger, O.,  
26 Tunyasuvunakool, K., Bates, R., Žídek, A., Potapenko, A., Bridgland, A., Meyer, C., Kohl, S. A.

- 1 A., Ballard, A. J., Cowie, A., Romera-Paredes, B., Nikolov, S., Jain, R., Adler, J., Back, T., and
- 2 Hassabis, D. (2021) Highly accurate protein structure prediction with AlphaFold. *Nature* 596,
- 3 583–589.
- 4 (17) Schell, M. A. (1993) Molecular biology of the LysR family of transcriptional regulators.
- 5 *Annu. Rev. Microbiol.* 47, 597–626.
- 6 (18) Liu, G. F., Wang, X. X., Su, H. Z., and Lu, G. T. (2021) Progress on the GntR family
- 7 transcription regulators in bacteria. *Yi Chuan* 43, 66–73.
- 8 (19) Chen, J., and Xie, J. (2011) Role and regulation of bacterial LuxR-like regulators. *J. Cell.*
- 9 *Biochem.* 112, 2694–2702.
- 10 (20) Krell, T., Molina-Henares, A. J., and Ramos, J. L. (2006) The lclR family of transcriptional
- 11 activators and repressors can be defined by a single profile. *Protein Sci.* 15, 1207–1213.
- 12 (21) Mistry, J., Chuguransky, S., Williams, L., Qureshi, M., Salazar, G. A., Sonnhammer, E. L.
- 13 L., Tosatto, S. C. E., Paladin, L., Raj, S., Richardson, L. J., Finn, R. D., and Bateman, A. (2021)
- 14 Pfam: The protein families database in 2021. *Nucleic Acids Res.* 49, D412–D419.
- 15 (22) Thompson, M. G., Valencia, L. E., Blake-Hedges, J. M., Cruz-Morales, P., Velasquez, A.
- 16 E., Pearson, A. N., Sermeno, L. N., Sharpless, W. A., Benites, V. T., Chen, Y., Baidoo, E. E. K.,
- 17 Petzold, C. J., Deutschbauer, A. M., and Keasling, J. D. (2019) Omics-driven identification and
- 18 elimination of valerolactam catabolism in *Pseudomonas putida* KT2440 for increased product
- 19 titer. *Metab. Eng. Commun.* 9, e00098.
- 20 (23) Thompson, M. G., Pearson, A. N., Barajas, J. F., Cruz-Morales, P., Sedaghatian, N.,
- 21 Costello, Z., Garber, M. E., Incha, M. R., Valencia, L. E., Baidoo, E. E. K., Martin, H. G.,
- 22 Mukhopadhyay, A., and Keasling, J. D. (2020) Identification, Characterization, and Application
- 23 of a Highly Sensitive Lactam Biosensor from *Pseudomonas putida*. *ACS Synth. Biol.* 9, 53–62.
- 24 (24) Hampel, K. J., LaBauve, A. E., Meadows, J. A., Fitzsimmons, L. F., Nock, A. M., and
- 25 Wargo, M. J. (2014) Characterization of the GbdR regulon in *Pseudomonas aeruginosa*. *J.*
- 26 *Bacteriol.* 196, 7–15.

- 1 (25) Meadows, J. A., and Wargo, M. J. (2018) Transcriptional Regulation of Carnitine  
2 Catabolism in *Pseudomonas aeruginosa* by CdhR. *mSphere* 3.
- 3 (26) Cowles, C. E., Nichols, N. N., and Harwood, C. S. (2000) BenR, a XylS homologue,  
4 regulates three different pathways of aromatic acid degradation in *Pseudomonas putida*. *J.*  
5 *Bacteriol.* 182, 6339–6346.
- 6 (27) Jiménez, J. I., Miñambres, B., García, J. L., and Díaz, E. (2002) Genomic analysis of the  
7 aromatic catabolic pathways from *Pseudomonas putida* KT2440. *Environ. Microbiol.* 4, 824–  
8 841.
- 9 (28) Barrientos-Moreno, L., Molina-Henares, M. A., Ramos-González, M. I., and Espinosa-  
10 Urgel, M. (2022) Role of the Transcriptional Regulator ArgR in the Connection between Arginine  
11 Metabolism and c-di-GMP Signaling in *Pseudomonas putida*. *Appl. Environ. Microbiol.* 88,  
12 e0006422.
- 13 (29) Silva-Rocha, R., and de Lorenzo, V. (2012) Broadening the signal specificity of prokaryotic  
14 promoters by modifying cis-regulatory elements associated with a single transcription factor.  
15 *Mol. Biosyst.* 8, 1950–1957.
- 16 (30) Anderson, J. C., Dueber, J. E., Leguia, M., Wu, G. C., Goler, J. A., Arkin, A. P., and  
17 Keasling, J. D. (2010) BglBricks: A flexible standard for biological part assembly. *J. Biol. Eng.* 4,  
18 1.
- 19 (31) Monteiro, L. M. O., Arruda, L. C. M., Sanches-Medeiros, A., Martins-Santana, L., Alves, L.  
20 de F., Defelipe, L., Turjanski, A. G., Guazzaroni, M. A.-E., de Lorenzo, V. C., and Silva-Rocha,  
21 R. (2019) Reverse Engineering of an Aspirin-Responsive Transcriptional Regulator in  
22 *Escherichia coli*. *ACS Synth. Biol.* 8, 1890–1900.
- 23 (32) Möglich, A., Ayers, R. A., and Moffat, K. (2009) Structure and signaling mechanism of Per-  
24 ARNT-Sim domains. *Structure* 17, 1282–1294.
- 25 (33) Henry, J. T., and Crosson, S. (2011) Ligand-binding PAS domains in a genomic, cellular,  
26 and structural context. *Annu. Rev. Microbiol.* 65, 261–286.

- 1 (34) Li, G., and Lu, C.-D. (2016) Molecular characterization of LhpR in control of hydroxyproline  
2 catabolism and transport in *Pseudomonas aeruginosa* PAO1. *Microbiology (Reading, Engl)* 162,  
3 1232–1242.
- 4 (35) Conrad, R. S., Massey, L. K., and Sokatch, J. R. (1974) D- and L-isoleucine metabolism  
5 and regulation of their pathways in *Pseudomonas putida*. *J. Bacteriol.* 118, 103–111.
- 6 (36) Jobe, A., and Bourgeois, S. (1972) lac repressor-operator interaction. *J. Mol. Biol.* 69, 397–  
7 408.
- 8 (37) Geissler, J. F., Harwood, C. S., and Gibson, J. (1988) Purification and properties of  
9 benzoate-coenzyme A ligase, a *Rhodopseudomonas palustris* enzyme involved in the  
10 anaerobic degradation of benzoate. *J. Bacteriol.* 170, 1709–1714.
- 11 (38) Roberts, J. B., Nava, A. A., Pearson, A. N., Incha, M. R., Valencia, L. E., Ma, M., Rao, A.,  
12 and Keasling, J. D. (2023) Foldy: a web application for interactive protein structure analysis.  
13 *BioRxiv*.
- 14 (39) Eberhardt, J., Santos-Martins, D., Tillack, A. F., and Forli, S. (2021) Autodock vina 1.2.0:  
15 new docking methods, expanded force field, and python bindings. *J. Chem. Inf. Model.* 61,  
16 3891–3898.
- 17 (40) Trott, O., and Olson, A. J. (2010) AutoDock Vina: improving the speed and accuracy of  
18 docking with a new scoring function, efficient optimization, and multithreading. *J. Comput.*  
19 *Chem.* 31, 455–461.
- 20 (41) Grosdidier, A., Zoete, V., and Michielin, O. (2011) SwissDock, a protein-small molecule  
21 docking web service based on EADock DSS. *Nucleic Acids Res.* 39, W270-7.
- 22 (42) Grosdidier, A., Zoete, V., and Michielin, O. (2011) Fast docking using the CHARMM force  
23 field with EADock DSS. *J. Comput. Chem.* 32, 2149–2159.
- 24 (43) Cooper, S., Khatib, F., Treuille, A., Barbero, J., Lee, J., Beenen, M., Leaver-Fay, A., Baker,  
25 D., Popović, Z., and Players, F. (2010) Predicting protein structures with a multiplayer online  
26 game. *Nature* 466, 756–760.



- 1 (44) Koepnick, B., Flatten, J., Husain, T., Ford, A., Silva, D.-A., Bick, M. J., Bauer, A., Liu, G.,  
2 Ishida, Y., Boykov, A., Estep, R. D., Kleinfelter, S., Nørgård-Solano, T., Wei, L., Players, F.,  
3 Montelione, G. T., DiMaio, F., Popović, Z., Khatib, F., Cooper, S., and Baker, D. (2019) De novo  
4 protein design by citizen scientists. *Nature* 570, 390–394.
- 5 (45) Bryant, P., Pozzati, G., and Elofsson, A. (2022) Improved prediction of protein-protein  
6 interactions using AlphaFold2. *Nat. Commun.* 13, 1265.
- 7 (46) Gordillo Sierra, A. R., and Alper, H. S. (2020) Progress in the metabolic engineering of bio-  
8 based lactams and their  $\omega$ -amino acids precursors. *Biotechnol. Adv.* 43, 107587.
- 9 (47) Silva, R., Coelho, E., Aguiar, T. Q., and Domingues, L. (2021) Microbial Biosynthesis of  
10 Lactones: Gaps and Opportunities towards Sustainable Production. *Appl. Sci.* 11, 8500.
- 11 (48) Ham, T. S., Dmytriv, Z., Plahar, H., Chen, J., Hillson, N. J., and Keasling, J. D. (2012)  
12 Design, implementation and practice of JBEI-ICE: an open source biological part registry  
13 platform and tools. *Nucleic Acids Res.* 40, e141.
- 14 (49) Chen, J., Densmore, D., Ham, T. S., Keasling, J. D., and Hillson, N. J. (2012) DeviceEditor  
15 visual biological CAD canvas. *J. Biol. Eng.* 6, 1.
- 16 (50) Hillson, N. J., Rosengarten, R. D., and Keasling, J. D. (2012) j5 DNA assembly design  
17 automation software. *ACS Synth. Biol.* 1, 14–21.
- 18 (51) Gibson, D. G., Young, L., Chuang, R.-Y., Venter, J. C., Hutchison, C. A., and Smith, H. O.  
19 (2009) Enzymatic assembly of DNA molecules up to several hundred kilobases. *Nat. Methods*  
20 6, 343–345.
- 21 (52) LaBauve, A. E., and Wargo, M. J. (2012) Growth and laboratory maintenance of  
22 *Pseudomonas aeruginosa*. *Curr. Protoc. Microbiol. Chapter 6*, Unit 6E.1.
- 23 (53) Rand, J. M., Pisithkul, T., Clark, R. L., Thiede, J. M., Mehrer, C. R., Agnew, D. E.,  
24 Campbell, C. E., Markley, A. L., Price, M. N., Ray, J., Wetmore, K. M., Suh, Y., Arkin, A. P.,  
25 Deutschbauer, A. M., Amador-Noguez, D., and Pfleger, B. F. (2017) A metabolic pathway for  
26 catabolizing levulinic acid in bacteria. *Nat. Microbiol.* 2, 1624–1634.

- 1 (54) Incha, M. R., Thompson, M. G., Blake-Hedges, J. M., Liu, Y., Pearson, A. N., Schmidt, M.,
- 2 Gin, J. W., Petzold, C. J., Deutschbauer, A. M., and Keasling, J. D. (2020) Leveraging host
- 3 metabolism for bisdemethoxycurcumin production in *Pseudomonas putida*. *Metab. Eng.*
- 4 *Commun.* 10, e00119.
- 5 (55) Lee, T. S., Krupa, R. A., Zhang, F., Hajimorad, M., Holtz, W. J., Prasad, N., Lee, S. K., and
- 6 Keasling, J. D. (2011) BglBrick vectors and datasheets: A synthetic biology platform for gene
- 7 expression. *J. Biol. Eng.* 5, 12.